Magnetic and electronic properties of HOPG/MoF$_6$ graphite intercalation compounds: An ESR study

D. Vaknin and D. Davidov

Racah Institute of Physics, Hebrew University of Jerusalem, Israel

H. Selig

Institute of Chemistry, Hebrew University of Jerusalem, Israel

Y. Yeshurun

Department of Physics, Bar-Ilan University, Ramat Gan, Israel

The diamagnetic MoF$_6$ molecule intercalates into graphite (HOPG) according to the reaction nC + MoF$_6$ → C$_n^{+x}$(MoF$_6^-$)$_x$(MoF_6)$_{1-x}$. Combination of ESR and magnetic susceptibility measurements indicate that the charge transfer is incomplete with $x \sim 0.2$. The system HOPG/MoF$_6$ is unique in that ESR resonances due to both the $4d^1$ intercalant species (MoF$_6^-$) and conduction carriers can be detected. The ESR spectra of stage III exhibit an additional resonance which is probably associated with graphite interior layers.

I. INTRODUCTION

The electron spin resonance (ESR) spectra of graphite intercalation compounds (GIC) have been extensively studied during the past several years.[1–5] Generally speaking, the ESR spectra in these compounds originate either with electron spins localized on the intercalant layers in the case of magnetic intercalant species[5,6] or from conduction carrier spins confined to the graphite layers in the case of nonmagnetic intercalants.[1–3] This paper reports on the magnetic and electronic properties of the HOPG/MoF$_6$ GIC with emphasis on the ESR measurements. We have observed, for the first time in any GIC, coupled resonance modes due to the paramagnetic intercalant species and the conduction carriers. Analysis of the ESR data together with a preliminary susceptibility study enables us to extract important information on the charge transfer, exchange mechanism, and the c-axis diffusion of the conduction carriers.

II. EXPERIMENTAL RESULTS

A. Sample preparation and characterization

The intercalation of MoF$_6$ into powdered graphite has been reported previously.[7] Here we report the intercalation of MoF$_6$ into HOPG for the first time. The intercalation process was carried out using slabs of HOPG of approximate dimensions $8 \times 3 \times 0.5$ mm in contact with liquid MoF$_6$ inside a reactor. Prior to the intercalation the HOPG slabs were pumped overnight at 300 °C to eliminate adsorbed gases. The MoF$_6$ was sublimed repeatedly using dry ice to eliminate HF. The intercalation is a relatively slow process possibly related to the low electron affinity of MoF$_6$. This enables us to monitor continuously the intercalation of HOPG/MoF$_6$ using an ac contactless conductivity technique.[8] An example for the normalized specific conductivity of HOPG/MoF$_6$ as a function of the exposure time is given in Fig. 1. As can be clearly seen from Fig. 1, the product of the in-plane conductivity σ and the sample thickness t increases stepwise upon intercalation of HOPG with MoF$_6$. The "plateaus" in

Fig. 1 (see points "b" and "c" in Fig. 1) correspond to mixtures of stages but a well-defined stage I at the end of the intercalation process (point "a"). This was confirmed by (00l) x-ray diffraction measurements obtained by interrupting the intercalation process and transferring the sample into a special sample holder for the CuKα x-ray study. These studies indicate a repeat distance (in Å) given by $d = 3.35 + (n - 1)d_s$, where n is the stage and $d_s = 8.35$–8.45Å with some variations from sample to sample. Results for pure stages I and III are shown in Fig. 2. The relative sample thickness t/t_0 was measured with a micrometer for stages I and III to be 2.3 ± 0.1 and 1.5 ± 0.1, respectively, consistent with the x-ray study. These values enable us to estimate the room temperature normalized conductivities σ/σ_0 to be 5.5 ± 0.5 and 9 ± 1 for stages I and III, respec-
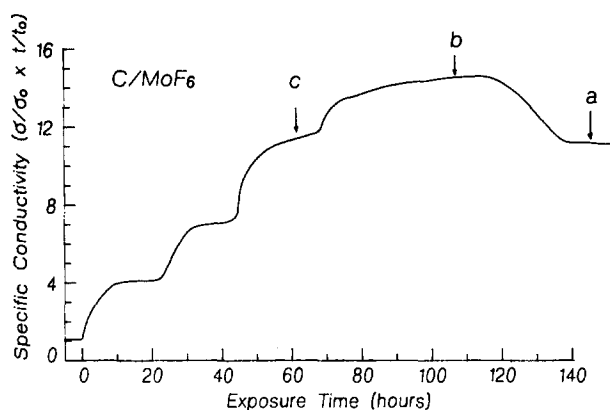

FIG. 1. The in-plane specific conductivity $(\sigma/\sigma_0)(t/t_0)$ of HOPG/MoF$_6$ as a function of exposure time to MoF$_6$. σ and t represent the in-plane conductivity and the sample thickness, respectively; σ_0 and t_0 are the same parameters for the initial HOPG. The arrows a, b, and c indicate the times at which the intercalation process was interrupted for x-ray (00l) analysis. Point a corresponds to pure stage I; points b and c correspond to mixture of stages (point b, for instance, corresponds to a mixture of stages I and II with a small amount of stage III).
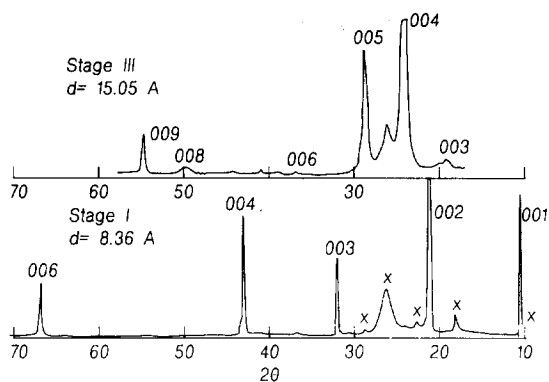
FIG. 2. X-ray (00l) diffraction pattern of HOPG/MoF$_6$ (stages I and III). Lines marked x arise from the sample holder.

tively, from Fig. 2. Thus HOPG/MoF$_6$ GIC exhibit relatively high in-plane conductivity. We believe that the jumps in the conductivity vs the exposure time correspond to noncontinuous charge transfer associated with weight uptake and filling of the intercalant layers. Apparently, the variation of the sample thickness upon intercalation does not play a very important role, as the transformation from stage II to stage I (Fig. 1) is associated with a decrease of the specific conductivity while t/t_0 increases.

B. ESR results

Samples for the ESR (or susceptibility) studies were sealed into quartz tubing under a helium atmosphere on a vacuum line following (00l) x-ray diffraction. These samples are stable and retain the same magnetic properties for a period of several weeks. The ESR measurements were carried out at X-band over the temperature range between 1.5 and 300 K. Figure 3 exhibits the ESR spectra of HOPG/MoF$_6$ at various temperatures for a stage I compound and for a magnetic field H parallel to the c axis ($H||C$). Two signals are clearly seen (signal d and signal c_1 in Fig. 3). At very low temperatures ($T \simeq 6$ K) the positions of these signals correspond to $g_d = 1.6 \pm 0.05$ and $g_{c1} = 1.89 \pm 0.01$, respectively. The position of signal c_1($g_{c1} = 1.89$) is practically angularly independent, but signal d shows some angular dependence of 150 G by rotating the c axis with respect to the magnetic field (Fig. 4). This corresponds to an angular dependence of $g_{||} - g_{\perp} = 0.05$. The angular dependence of signal d is, however, significantly smaller than its linewidth ($\Delta H \sim 230$ G).

An interesting feature of Fig. 3 is the decrease of the ESR intensities of signals d and c_1 with increasing temperature. Note, however, while signal d practically disappears above $T = 60$ K, signal c_1 could be observed even at room temperature. An additional interesting feature is the line position. The position of signal d is almost temperature independent while the position of signal c_1 changes from $g = 1.89 \pm 0.01$ to 1.99 ± 0.01 upon increasing the temperature from $T = 4$ to 300 K. This shift in the line position is associated with significant linewidth narrowing. Figure 5(b) exhibits the g shift of line c_1 vs temperature measured with respect to $g = 2$.

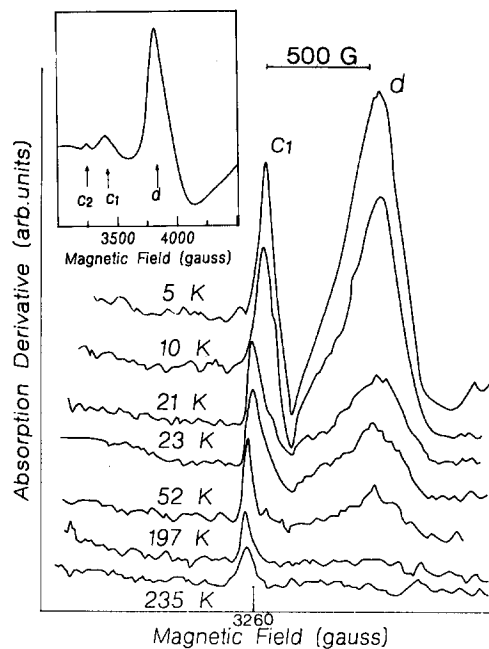While stages I and II of HOPG/MoF$_6$ GIC show very

FIG. 3. ESR spectra of stage I HOPG/MoF$_6$ for H||C and at various temperatures. Two signals d and c_1 are clearly seen. The inset shows the ESR spectrum of stage III at $T = 6$ K. This spectrum exhibits an additional line, c_2.

similar spectra (see Fig. 3), the low temperature ESR spectra of stage III compounds exhibit an additional line at $g = 2$. The insert of Fig. 3 shows the ESR spectra of stage III HOPG/MoF$_6$ at $T = 6$K. Although the intensity of this additional signal is very small, we definitely identify the same signal in several HOPG/MoF$_6$ samples of stage III.

C. Magnetic susceptibility

The susceptibility of a mixture of stages of HOPG/MoF$_6$ was measured using a SQUID in the temperature range 6 K $< T <$ 80 K with the magnetic field H perpendicular to the c axis. The results [Fig. 5(a)] could be fitted to the formula

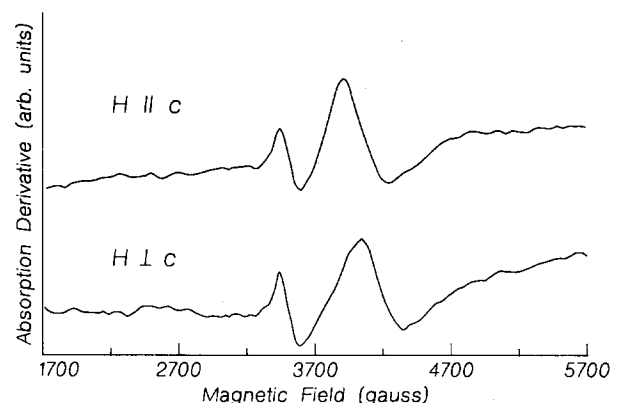$$\chi = \frac{N\mu_{\text{eff}}^2}{3K_B(T+\theta)} + \chi_0, \tag{1}$$

FIG. 4. The angular dependence of the ESR spectrum of HOPG/MoF$_6$ stage II at $T = 6$ K.

where μ_{eff} is the effective magnetic moment, N is the number of MoF$_6$ molecules as estimated from the weight uptake, χ_0 is the temperature independent susceptibility, and K_B is the Boltzman constant. We found $\mu_{eff} = 0.63\,\mu_B$, $\theta = 3$ K, and $\chi_0 = 1.66 \times 10^{-3}$ emu/mol Oe. The large value of the temperature independent susceptibility is not clearly understood yet. It may be only partially associated with the large orbital paramagnetism of the intercalant molecules,[9] or Pauli susceptibility due to the conduction carriers.

III. DISCUSSION

The neutral MoF$_6$ molecule is diamagnetic with a $4d^0$ electronic configuration. Upon intercalation the following chemical reaction occurs:

$$nC + MoF_6 \rightarrow C_n^{+x}(MoF_6^-)_x(MoF_6)_{1-x}. \qquad (2)$$
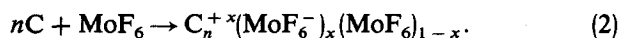
This reaction leads (partially) to the formation of MoF$_6^-$ ions in which the oxidation state of the molybdenum is $+5$ (Mo^{+5}) with a $4d^1$ electronic configuration. Thus, the chemical reaction leads to charge transfer which results in the formation of local magnetic moments on the intercalant species and mobile spins (holes) on the graphite layers. We believe that the spectra in Figs. 3 and 4 are due to coupled resonance modes associated with these two spin species. Indeed the different temperature dependence of the intensity strongly supports the idea that signals d and c_1 originate from different spin species. The coupling is provided by exchange interaction of the form $J\,\mathbf{S}\cdot\mathbf{s}$, where $\mathbf{S}$ is the spin of the Mo^{+5} ion while $\mathbf{s}$ is the spin of the conduction carrier. A similar problem has been treated extensively in the case of metals.[10-13] In the limit of weak exchange coupling, we identify signal d in Fig. 3 with the paramagnetic MoF$_6^-$ (V) ions and signal c_1 as dominated by the conduction carriers. This identification is supported by the following observations: (a) The intensity of signal d decreases with increasing temperature, roughly as $\sim 1/T$, as expected for localized paramagnetic ions. The properties of signal d are consistent with the ESR of Mo^{+5} in various insulating solids.[14,15] It has been demonstrated[14,15] that Mo^{+5}($4d^1$) in insulators exhibit slightly anisotropic g values and resolved hyperfine interactions due to Mo^{97} and Mo^{95} isotopes. The relatively large linewidth of signal d can be explained, therefore, as due to unresolved hyperfine interaction. The relative broad line compared to the anisotropy of the g value, does not allow detailed analysis of line d. The slight differences between the ESR g value as compared to the previous ESR studies[14,15] are probably due to different local environments leading to different crystal field parameters. (b) Signal c_1 is believed to be associated with conduction carriers. In such a case, one expects the signal intensity to be almost temperature independent according to the Pauli law. However, as will be shown below we are able to explain both the temperature dependence of the position of line c_1 as well as its intensity in the frame of the weak exchange coupling model.

Due to the exchange interaction the position of signal c_1 is exchange shifted and in the molecular field approximation the g shift Δg_c, is given by[13]

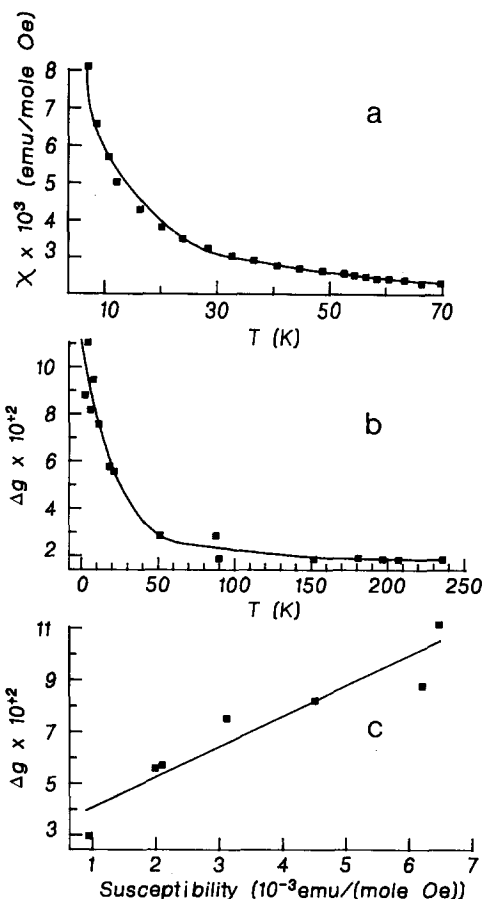$$\Delta g_c = g_c - 2 = J\chi_d/2\mu_B^2 N, \qquad (3)$$

FIG. 5. (a) The susceptibility of a mixture of stages (stages I, II, and III) of HOPF/MoF$_6$ vs temperature. (b) The g shift Δg_c of the line c_1 vs temperature. The g shift was measured with respect to $g = 2$ (c) A plot of Δg_c vs the susceptibility with the temperature as implicit parameter. The solid line represents the best fit.

where χ_d is the spin susceptibility of the intercalant ions. As seen, Δg_c is proportional to χ_d with a coefficient which depends on the exchange parameter J. Equation (3) is in agreement with Fig. 5(c) where the experimental Δg_c was plotted against the susceptibility of HOPG/MoF$_6$. Using Eq. (3) and our data in Fig. 5(c), we have extracted a negative (antiferromagnetic) exchange parameter $J = (-0.9 \pm 0.2)$ meV. The negative exchange interaction is consistent also with the enhancement of signal c_1 at low temperature according to a mechanism suggested previously by Pifer and Longo.[11] They have pointed out that due to overlap (hybridization) of two resonance lines, the effective alternating field might be enhanced or reduced depending on the sign of the coupling constant. This mechanism is analogous to the enhancement of the nuclear magnetic resonance in ferromagnets.[16] It is associated with the fact that the transverse magnetization of signal d, which is coupled to the magnetization of signal c_1 via the exchange, has a component which oscillates in-phase with the external rf field H_{rf}. The enhancement of the rf field is roughly given by $H_{rf}^2 \cdot (1 + \lambda\chi_d')^2$ where χ_d' is the amplitude of the dispersion line of signal d at the position of signal c_1. In our case, both χ_d' and λ are negative leading to enhancement. Furthermore, χ_d' is proportional to the static

susceptibility, and consequently the enhancement factor decreases with increasing temperature. This is in qualitative agreement with the decrease of the intensity of signal c_1 upon increasing the temperature (Fig. 3).

The value of g_d associated with the Mo^{+5} ions is almost unaffected by the exchange mechanism in this limit of very small exchange interaction and the relatively small Pauli susceptibility associated with the conduction carriers. Knowledge of g_d enables us to estimate the effective magnetic moment of the Mo^{+5} ions assuming spin $S = \frac{1}{2}$ as follows:

$$\mu_{\mathrm{ESR}} = g_d \sqrt{S(S+1)} \mu_B = 1.4 \mu_B.$$

This value of μ_{eff} is significantly larger than the effective magnetic moment extracted from the susceptibility ($\mu_{\mathrm{eff}} = 0.63\ \mu_B$). This "discrepancy" can be resolved if the chemical reaction does not go to completion. The charge transfer coefficient $(\mu_{\mathrm{eff}}/\mu_{\mathrm{ESR}})^2 = (0.63/1.40)^2 = 0.2$, i.e., $\sim 20\%$ of the MoF$_6$ molecules undergo charge transfer. This number should be regarded with some caution, because our susceptibility measurements were done on mixtures of stages, while the charge transfer might be stage dependent.[3]

Probably the most interesting feature of our experimental results is the observation of two lines for stages I and II (which contain only bounding equivalent graphite layers) but the observation of three lines for stage III compounds. In stage III the graphite layers are nonequivalent and we can distinguish between bounding layers (adjacent to the intercalant layers) and interior layers. The resonance at $g_{c_2} \simeq 2$ found at low temperature for stage III compounds is attributed, therefore, to the graphite interior layers. This resonance is angularly independent and, thus, has very similar properties to the ESR of the conduction carriers in nonmagnetic intercalant systems.[1–4] We note that in "pure" HOPG the ESR is very anisotropic compared to its linewidth.[1] This strongly supports the idea that there is significant charge transfer even to interior graphite layers. The charge transfer to interior layers is consistent with theoretical work of Safran[17] and others[18,19] who have demonstrated the existence of long range (nonexponential) charge screening of the "charged" intercalant layers.

The observation of two different resonance lines associated with graphite bounding layers and graphite interior layers, respectively, strongly suggest that (a) the exchange interaction mechanism is of short range and does not affect the carriers on interior layers and (b) the rate of the conduction carriers hopping along the c axis is very slow. We note that according to the theory for motional narrowing,[21] one expects the two ESR lines associated with the conduction carriers to merge into a single line for a "fast" c axis hopping rate relative to the difference in the resonance frequencies of these two lines. Thus, our experiment suggests that the hopping rate is a "slow" process. We estimate a lower limit to the hopping time τ_c to be $\tau_c > 10^{-9}$ s.

IV. SUMMARY

(1) HOPG/MoF$_6$ is the only system known to us for which the resonances due to the intercalant species and the conduction carriers (both associated with the charge transfer) could be detected. The observation of the later resonance is probably due to the relatively small exchange and spin-orbit broadening mechanism expected for the $4d$ series.[4]

(2) The resonance properties of signal d, indicate a $4d^1$ electronic configuration appropriate to Mo^{+5} (i.e., MoF$_6^-$). However, the charge transfer is not complete; only $\sim 20\%$ of the MoF$_6$ molecules undergo charge transfer. These results are in qualitative agreement with previous results on C/ AsF$_5$.[3,20]

(3) The ESR spectra of stages I and II can be explained by using a weak exchange coupling mechanism. A value of $J = -0.9 \pm 0.2$ meV was extracted from our data. Although this value of the exchange should be regarded with caution because the susceptibility was measured on a mixture of stages, the magnitude is correct. The magnitude of this exchange parameter is smaller by several orders of magnitude than the ion conduction electron exchange interaction in metals (0.1 to 1 eV)[12,13] This strongly supports the idea that overlap of the wave functions in the intercalated compounds is rather small and the conduction carriers are mainly confined to the graphite layers. The small value of J could also be due to the fact that the Mo is well shielded from the environment by the surrounding fluorine atoms and therefore does not interact much with the conduction carriers.

[1]M. S. Dresselhaus and G. Dresselhaus, Adv. Phys. **30**, 139 (1981).
[2]S. K. Khanna, E. R. Falardeau, A. J. Heeger, and J. E. Fischer, Solid State Commun. **25**, 1059 (1978).
[3]B. R. Weinberger, J. Kaufer, A. J. Heeger, J. E. Fisher, M. Moran, and N. A. W. Holzwarth, Phys. Rev. Lett. **41**, 1417 (1978).
[4]D. Davidov, O. Milo, I. Palchan, and H. Selig, Synth. Metals **8**, 83 (1984).
[5]D. Vaknin, D. Davidov, H. Selig, V. Zevin, I. Felner, and Y. Yeshurun, Phys. Rev. B **31**, 3212 (1985).
[6]M. Suzuki, M. Murata, and H. Suematsu, Synth. Metals **6**, 1973 (1983); R. Nishitani, K. Ohmatsu, H. Suematsu, and M. Murata, *ibid.* **6**, 185 (1983).
[7]A. Hamwi, Ph. Touzain, and L. Bonnetain, Mater. Sci. Eng. **31**, 95 (1977).
[8]C. Zeller, A. Denenstein, and G. M. T. Foley, Rev. Sci. Instrum. **50**, 602 (1979).
[9]S. A. Safran, Phys. Rev. B **30**, 421 (1984).
[10]H. Hasegawa, Progr. Theor. Phys. (Kyoto) **21**, 483 (1959).
[11]J. H. Pifer and R. T. Longo, Phys. Rev. B **4**, 3797 (1971).
[12]S. Schultz, D. R. Fredkin, B. L. Gehman, and M. R. Shanabarger, Phys. Rev. Lett. **21**, 1297 (1973).
[13]R. H. Taylor, Adv. Phys. **24**, 681 (1975).
[14]R. T. Kyi, Phys. Rev. **128**, 151 (1962).
[15]T. T. Chang, Phys. Rev. A **136**, 1413 (1964).
[16]A. M. Portis and R. H. Lindquist, in *Magnetism IIA*, edited by G.T. Rado and H. Suhl (Academic, New York, 1963).
[17]S. A.Safran and D. R. Hamann, Phys. Rev. B **22**, 606 (1980).
[18]L. Pietronero, S. Strassler, H. R. Zeller, and M. J. Rice, Phys. Rev. Lett. **41**, 763 (1978).
[19]S. A. Safran and D. R. Hamann, Phys. Rev. B **23**, 565 (1981).
[20]J. W. Milliken and J. E. Fischer, J. Chem. Phys. **78**, 5800 (1983).
[21]A. Abragam, *The Principles of Nuclear Magnetism* (Oxford University, Oxford, 1961).